

STRENGTHENING AND MONITORING TECHNIQUES FOR ASR-AFFECTED FOOTING OF BRIDGE PIER

Kazutoshi Okuyama^{1,*}, Kouji Ishii², Yoshinori Okuda³, Kazuyuki Torii⁴

¹P.S. Mitsubishi Construction Co., Ltd., 1-8-30 Tenmabashi, Kita-Ku, OSAKA, Japan

²P.S. Mitsubishi Construction Co., Ltd., 2-5-24 Harumi, Chuo-Ku, TOKYO, Japan

³ARS Consultants Co., Ltd., 2-1-1 Izuminode-Machi, KANAZAWA, Japan

⁴Kanazawa University, Kakuma-Machi, KANAZAWA, Japan

Abstract

Concrete deterioration resulting from the alkali silica reaction (ASR) is commonly identified in above ground locations on structures, as typified by the deterioration of columns and beams of bridge piers. When ASR damage is identified, countermeasures are implemented. However, there have been few reports on the deterioration of below ground bridge pier footings and no measures for the control of such deterioration have been established. This report describes a bridge pier footing that has suffered ASR deterioration, the countermeasure taken to combat the deterioration and the results of monitoring the effect of the countermeasure in controlling ASR-induced concrete expansion. In this case, the countermeasure adopted was the strengthening method with prestressing steel (PC confined method), in which tensioned prestressing steel strand was wound around the periphery of the footing and the footing was laid out with tensioned vertical prestressing steel bar.

Keywords: Bridge pier footing, Strengthening method with prestressing steel (PC confined method), Expansion-controlling effect, Monitoring

1 INTRODUCTION

In recent years, many deterioration examples of the structure by the alkali silica reaction (ASR) are reported, and various measure methods of construction are enforced [1]. Conventional concerns related to concrete affected by ASR were loss of compressive strength, reduced elastic modulus and loss of bonding between steel bars and the cover concrete. In addition to these earlier concerns, there have been recent reports of other problems: continuing expansion of concrete due to the ASR over the long term; development of cracking deep inside the concrete due to continuing expansion of the concrete; and fracturing of stirrup or bent-up steel bars at their bends. These deterioration modes have adverse effects on the load-carrying capacity of structures and can become a major problem [2].

Identification of concrete deterioration resulting from the ASR has generally involved above ground structures, such as the columns and beams of bridge piers, abutments, retaining walls, culverts and rock fall sheds. However, there have been few reports on the deterioration of bridge pier footings, which are buried under the ground. Checks on the condition of pier footings with ASR are extremely important [3,4]. The deteriorated bridge pier footing described in this report was discovered during excavations to install a support structure for the superstructure and place new concrete in a beam of bridge piers that had suffered ASR deterioration. This report describes the deterioration of the footing, the basic concept for the countermeasures to combat the deterioration and the post-implementation monitoring of the footing.

2 OUTLINE OF THE BRIDGE

Table 1 is an outline of the bridge with the ASR-damaged pier footing repaired and reinforced in this work. Figure 1 is an overall view of the bridge and Figure 2 is a bridge pier before strengthening. Figure 3 is a general drawing of the bridge pier.

Table 2 shows mix proportions of concrete used in the footings of the bridge.

The pier was also found damaged by ASR at its lower part of the column. As known to be dependent to a large extent on groundwater condition, ASR deterioration in other footings varied in degree of severity, ranging from very minor one.

* Correspondence to: k-okuyama@psmic.co.jp

3 INSPECTION OF DETERIORATED FOOTING

3.1 Visually observed deterioration

Excavation was carried out as deep as the top surface of the leveling concrete surrounding the base of the footing, as shown in Figure 2. Cracks were present over the whole top surface of the footing. The cracks measured about 5 mm in width. The cracking was particularly prominent at edges where the top face and sides of the footing met, and the concrete was weakened in places. Some concrete had peeled off at the edges and some steel bars were exposed as a result of this edge weakening and due to the effects of excavation.

Toward the top of the footing sides, cracks had developed with the same density as on the top of the footing. Edge cracks that had developed in the horizontal direction were especially prominent, measuring 20 mm in maximum width. These cracks appeared to be the result of fracturing of most of the reinforcing bars in this region. Toward the bottom of the footing, these side cracks tended to decrease in number and width.

After removing the cover concrete around the upper region of the footing periphery, most of the exposed bends of the steel bars were found to be fractured. Figure 4 shows the deteriorated concrete on the top of the footing. Figure 5 shows the deteriorated concrete around the top edges and on the sides of the footing.

3.2 Deterioration of core samples

Guided by the results of the visual inspection described above, cores measuring 100 mm in diameter and about 2.5 m long were taken from the sampling points shown in Figure 6, two each in the horizontal and vertical directions. The horizontal cores were taken with fractured 20-30 cm under the concrete surface. In the fractured cross section, water permeation was observed.

Further, white deposits were observed not only around coarse aggregate particles but also inside the aggregate particles in the cores. These deposits seemed to be gels formed through reaction with alkalis that permeated the aggregates after they cracked due to the ASR. Figure 7 shows a cross section of one core.

3.3 Compressive strength and elastic modulus of concrete

The compressive strength and elastic modulus of the sampled concrete were measured so as to examine the concrete's mechanical properties. Core No. 1 was used to examine mechanical properties near the surface of the footing and Core Nos. 2, 3 and 4 at a depth of about 1.3 m from the footing surface, respectively. Figure 8 shows the relationship between concrete compressive strength and the ratio of the elastic modulus to compressive strength (E_c/f_c). Every test specimen had a compressive strength approximating the specified design strength (21 N/mm²), but the elastic modulus was considerably lower. In fact, the elastic modulus of concrete from near the surface of the footing was found to be 45% of that specified in the Specifications for Highway Bridges. A correlation was identified between the test results and the visual inspection results.

3.4 Residual expansion of concrete

With a view to confirming the residual expansion of the concrete, accelerated curing tests were conducted. For the curing, each four specimens were prepared for two methods: immersion in 80±2°C 1N-NaOH solution; and immersion in 50±2°C saturated NaCl solution. These specimens were sampled from Core Nos. 3 and 4, which were used for the above-mentioned measurement of compressive strength and elastic modulus. They were taken near the surface of the footing and at a depth of about 2.0 m below the surface of the footing. Figures 9 and 10 show the results of the residual expansion test.

The results for the immersion in 1N-NaOH solution revealed that specimens sampled from Core No. 3 near the surface and at a depth of about 2.0 m expanded considerably. The expansion ratio at a curing age of 28 days reached as much as 0.35%. Although expansion ratios for specimens sampled from Core No. 4 were smaller than those from Core No. 3, the figure for the specimen sampled from Core No. 4 near the surface reached 0.2% at a curing age of 28 days.

The curing in saturated NaCl solution yielded unclear results for every test specimen. Although the results were somewhat different for the different test methods, it was clear that both NaOH and NaCl solutions would take longer to permeate into the core of the 100-mm-diameter test sample than the specified curing time until the measurements were taken. Since neither solution permeated into the core of the test specimens, the footing concrete was thought to have high residual expansivity.

4 STRENGTHENING PLAN

The visual inspection found many main steel bars in the footing fractured at their bends in the direction of bridge axis and in the transverse direction. Since the compressive strength of the footing concrete remained close to the design strength as a whole, aside for one weakened region, and concrete expansion toward the bottom of the footing sides had been constrained by leveling concrete since construction (See Figure 3), the main reinforcing bars at the bottom of the footing were thought to be sound. It was judged possible to recover the load-carrying capacity of the footing by taking appropriate measures to counter concrete expansion caused by the ASR. The basic plan adopted in developing the countermeasures was that the footings should recover their structural function and that an implementation method should be chosen that would control the ASR-induced expansion of concrete.

The strengthening method with prestressing steel (PC confined method) has a good track record in the strengthening of bridge piers against ASR-induced expansion of concrete, so it was selected to recover the integrity of the structure. Prestressing steel was wound around the periphery of the footing and tensioning vertical prestressing steel was added to the footing. Table 3 shows mechanical properties of the steel used for the strengthening.

5 STRENGTHENING PROCESS

5.1 Removal of footing concrete and reinforcing bar strengthening

The concrete at the top and sides of the footing within 1 m of each top end was chipped away to a depth of about 200 mm by using breaker and water jet to expose the steel bars. Because the visual inspection had identified fractured steel bars at these bends, an anticorrosion product was applied to the steel bars and new bars were spliced as splints to the fractured bars. Figure 11 shows the footing after the concrete had been chipped away.

5.2 Prestressing around the periphery of footing and in the vertical direction

To control the ASR-induced expansion of the concrete, prestressing steel was wound around the periphery of the footing and also laid in the vertical direction. The steel was then tensioned. Prestressing steel bars (D32 mm) were used for the vertical prestressing to ensure the bonding between steel and concrete. At the bottom end of these prestressing steel bars, a 500 mm deep anchorage zone was provided and a nut was turned onto the end of the bar to enhance bonding. In addition, to distribute the prestressing force over a wide area, a 250 mm square anchorage plate was attached to the top end of the bar. It is known from a previous test on column members that confining at 30% of the yield of the prestressing steel generates a restraining pressure of 0.2 N/mm² which can confine concrete expansion [2]. The amount of prestress for the current test was determined as the number of prestressing steel bars capable of introducing a confining force of 0.2 N/mm².

The peripheral reinforcement was with prestressing steel strand (1S21.8 mm). To ensure pressure at the edges of the footing, these prestressing steel strands were wound with a minimum radius of 3.8 m. The level of the stress introduced was not less than 0.2 N/mm² as in the case of the vertical prestressing. Taking into account the possible rise in prestressing steel stress as ASR-induced expansion of concrete proceeds and in earthquakes, the effective tensioning force was set at 30-40% of the yield load of the steel. Figure 6 shows the layout of prestressing steel. Figures 12, 13 and 14 show the prestressing steel strand around the periphery of the footing and the vertical prestressing steel bar, respectively. Figure 15 shows bridge pier after the strengthening.

6 POST-STRENGTHENING MONITORING

The footing that had suffered deterioration because of the ASR was inspected, repaired and reinforced as described above. To confirm the effectiveness of the strengthening method used and to collect base data for the establishment of a standard strengthening method, the footing was monitored after completion of the work using various measuring instruments. Monitoring was done for about a year and a half (540 days), between May 2005 and October 2006. Monitoring is still ongoing and additional results will be presented at the conference of the 13th ICAAR.

6.1 Control of footing concrete expansion

Expansion of the footing concrete was measured by attaching crack displacement gauges to a selected crack on one of the sides of the footing. A relatively large crack was selected for this purpose and gauges were attached in both vertical and horizontal directions. Figure 16 shows crack displacement gauges, Figure 17 shows the change over time in crack width. The results revealed that

the crack width varied within a roughly constant range relative to the initial value (at the time of strengthening) and that crack width tended to decrease slightly during the summer.

6.2 Strain in vertical prestressing steel bars

To confirm the effect of the vertical prestressing steel bar on controlling expansion of the footing concrete, strain gauges were attached to the steel. Figure 18 shows the location of these strain gauges on the prestressing steel bars and steel bars. Figure 19 shows the change over time in strain in the vertical prestressing steel bar. As can be seen from these measurements, over time the strain tended to become compressive on the whole. The reason for this is thought to be as follows. Many micro cracks caused by the ASR were present in the concrete and these contracted elastically immediately after prestressing. Subsequently, however, these micro cracks were crushed, leading to a decrease in strain. This change was noticeable from spring through autumn. In contrast, the prestressing force increased from summer through winter.

6.3 Strain in steel bars

The initial visual inspection indicated that there was fracturing of the steel bars at the bends caused by the ASR-induced concrete expansion. To check the stress in the steel bars in the footing after strengthening, they were fitted with strain gauges. The strain gauges were attached to the inner and outer radii of the bends. Figure 20 shows the change over time in the strain in the steel bars. The strain at the bends tended to fall, as in the case of strain in the vertical prestressing steel bars.

7 CONCLUSIONS

The authors inspected a bridge footing that had suffered deterioration as a result of the ASR, a little-reported phenomenon. A strengthening method was devised, strengthening method with prestressing steel, and work carried out to reinforce the footing. To verify the effectiveness of the method selected, the strengthened footing was monitored. The results of monitoring indicate that the vertical prestressing force is tending to fall while strain at the bend in a steel bar is tending to become compressive. These trends point to overall contraction of the footing, which seems to be connected with deformation of micro cracks due to creep. It is planned to continue monitoring the change over time in strain.

The strengthening method with prestressing steel adopted here is known to control the effects of ASR-induced expansion in concrete columns, but its effectiveness for members such as footings has not yet been demonstrated. However, this prestressing technology is expected to prove effective for footings. The authors expect that the strengthening method adopted here will evolve into an established method based on the data collected through monitoring.

8 REFERENCES

- [1] Torii, K., Okuda, Y., Ishii, K., Satou, K. (1999): Reported Loading Test for ASR Damaged Concrete Columns Strengthened by PC Confined Method: Proceedings of the Japan Concrete Institute, Vol. 21, No. 2: 1051-1056
- [2] Ishii, K., Okuda, Y., Tanigawa, S., Torii, K. (2005): ASR mitigation-effect of repair and retrofitting methods against ASR damaged reinforced concrete columns: Concrete Journal, Vol. 43, No. 7: 42-50
- [3] Torii, K., Daidai, T. (2006): Strengthening and Monitoring Techniques of ASR Affected Bridge Piers: Proceedings of 22nd ARRB, Canberra: CD-R 10 pages
- [4] Torii, K., Okuyama, K., Kuzume, K., Sasatanai, T. (2007): Monitoring and Strengthening Methods of Bridge Pier Seriously Damaged by Alkali-silica Reaction: Proceedings of Inter Conf. on CONSEC'07, Tours, Vol. 1: 787-794

TABLE 1: Outline of the bridge.

Bridge name	Tokuda Nigo Bridge
Location	Noto Expressway in Ishikawa Prefecture
Year of completion	1980
Bridge type	Superstructure: 9-span prestressed concrete post-tensioned T-girder bridge Substructure: rectangular column overhanging bridge pier (spread foundation)
Bridge length	302 m
Bridge pier height	About 27 m

TABLE 2: Mix proportions of the concrete used in the footings of the bridge.

Design strength (N/mm ²)	Aggregate size (mm)	Fine aggregate type	Coarse aggregate type	Cement type	W/C (%)	Unit cement content (kg/m ³)	Alkali from cement (kg/m ³)
21 or 24	25 or 40	River sand or pit sand (non-reactive)	Crushed andesite stone (reactive*)	Normal portland cement	49--56	270--320	2.16--2.56

*: reactive minerals in andesite stone: cristobarite, volcanic glass
 **: Alkali in cement: around 0.8%

TABLE 3: Mechanical properties of steel used for the strengthening.

Type	Steel	Sectional area (mm ²)	Yield point (N/mm ²)	Tensile strength (N/mm ²)	Elongation (%)
Steel bar	SD345, D: 16 mm	198.6	345--440	490	18
Vertical prestressing steel	Prestressing steel bar, D: 32 mm	804.2	930	1080	6
Peripheral prestressing steel	Prestressing steel strand, 1S 21.8 mm	312.9	1600	1800	3.5



Figure 1: Overall view of the bridge.



Figure 2: Bridge pier before strengthening.

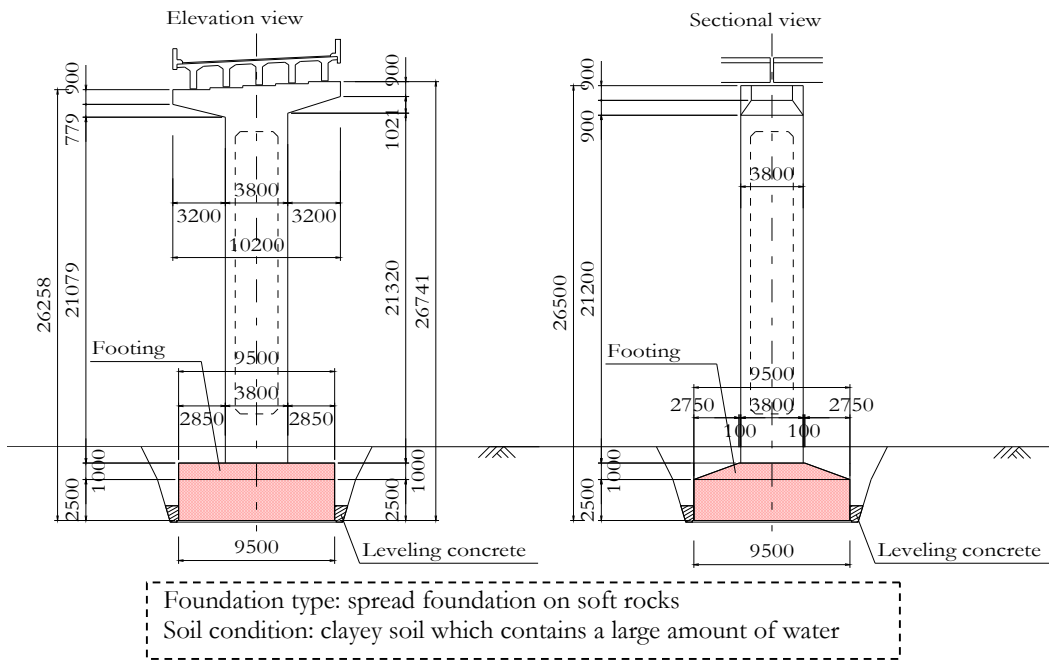


Figure 3: General drawing of the bridge pier.



Figure 4: Deteriorated concrete at the footing top.



Figure 5: Enlarged view of deteriorated concrete at the edge and sides of the footing top.

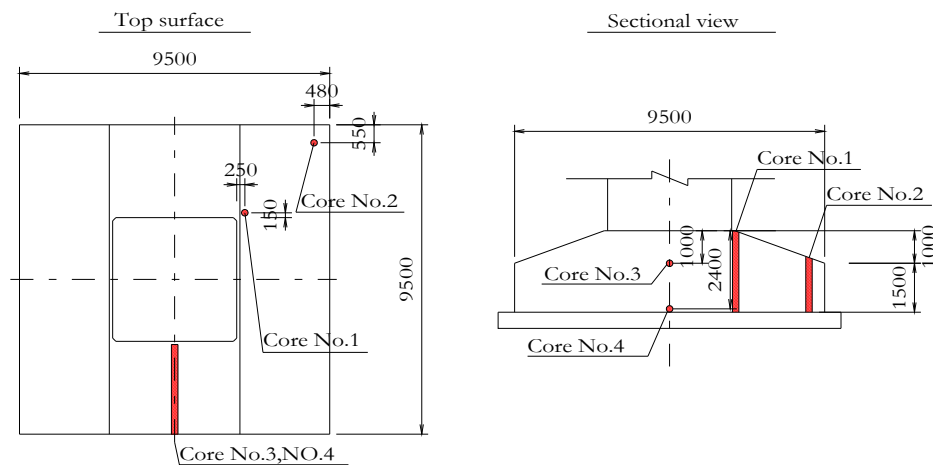


Figure 6: Core sampling points



Figure 7: Cross-sectional view of a core sample (ø100 mm).

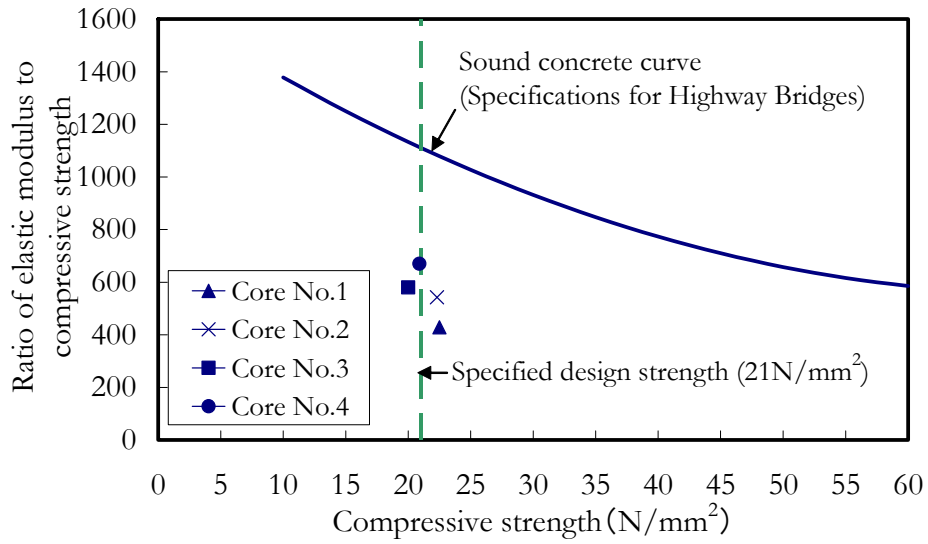


Figure 8: Relationship between the concrete compressive strength and the ratio of the elastic modulus to compressive strength (E_c/f_c).

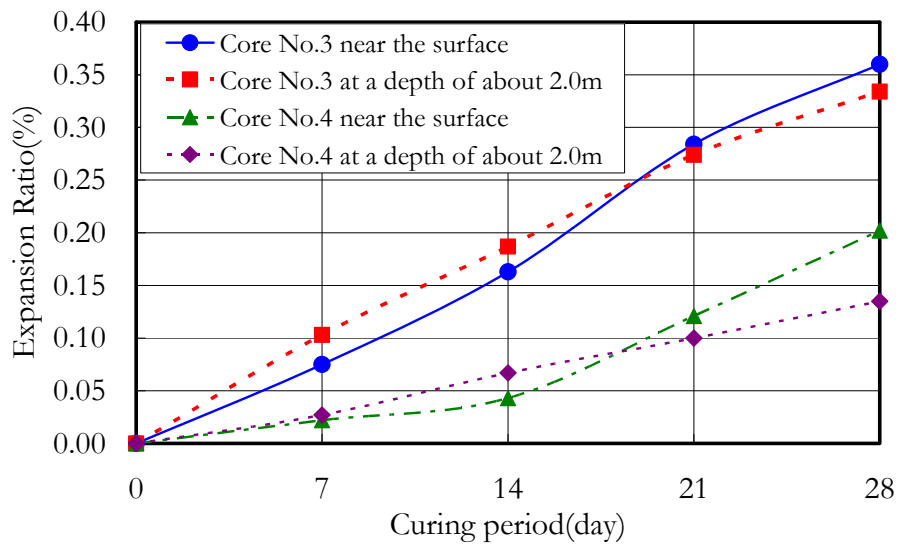


Figure 9: Results of accelerated curing test (immersed in $80\pm 2^\circ\text{C}$ 1N-NaOH solution).

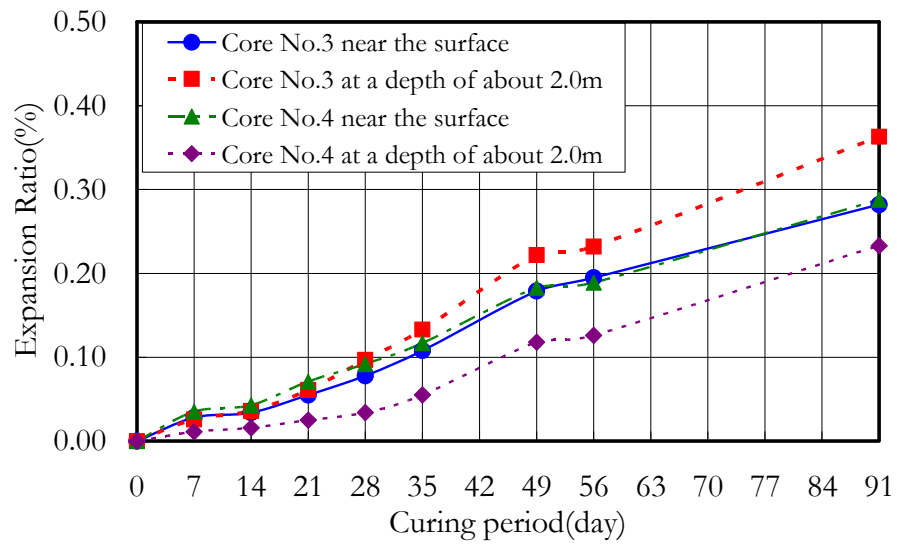


Figure 10: Results of accelerated curing test (immersed in $50\pm 2^\circ\text{C}$ saturated NaCl solution).



Figure 11: Footing after chipping away concrete.

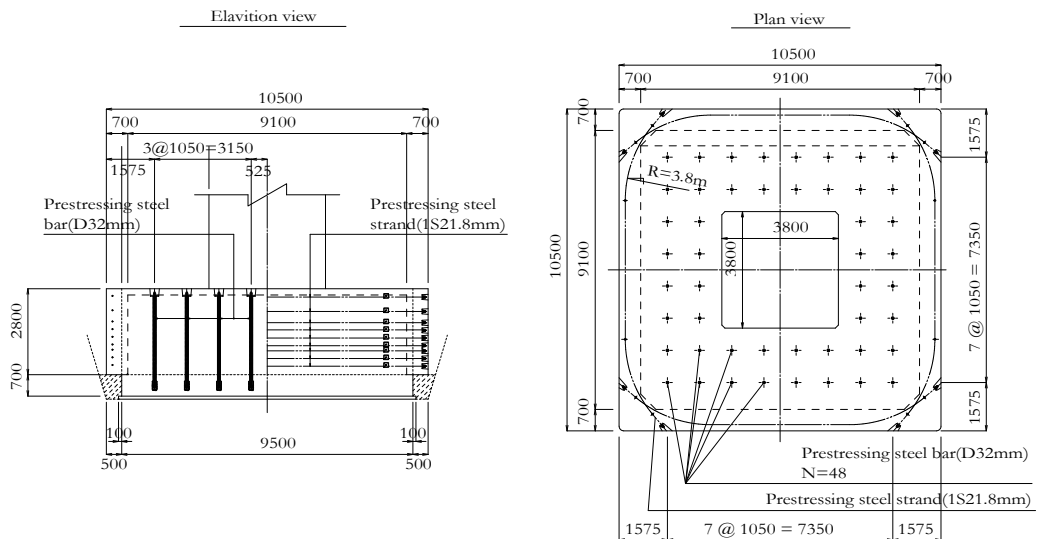


Figure 12: Layout of prestressing steel.



Figure 13: Layout of prestressing steel strand around periphery of footing.



Figure 14: Layout of vertical prestressing steel bar.



Figure 15: Bridge pier after the strengthening.



Crack displacement gauge
Figure 16: Crack displacement gauge.

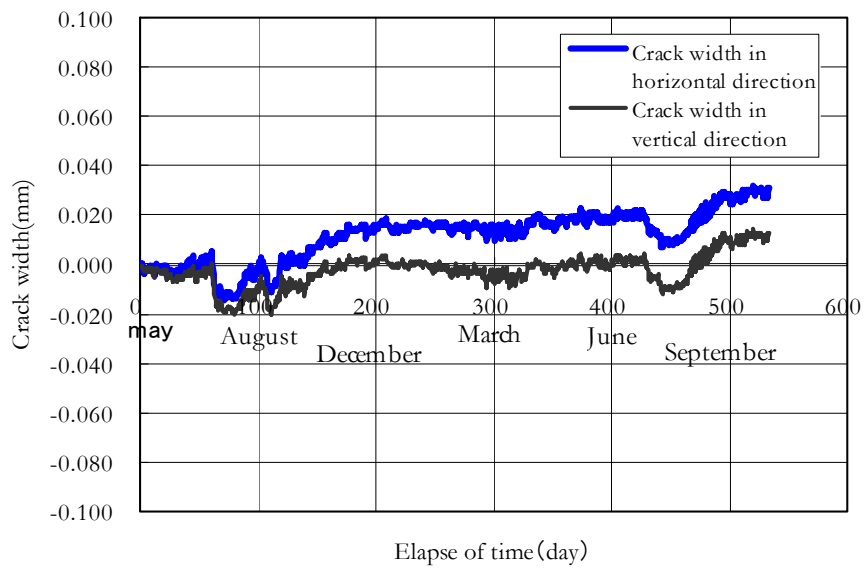


Figure 17: Change over time in crack width.

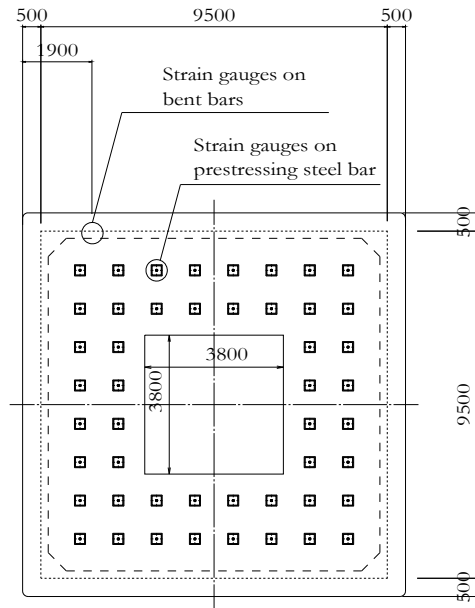


Figure 18: Location of strain gauges on prestressing steel bars and bent bars.

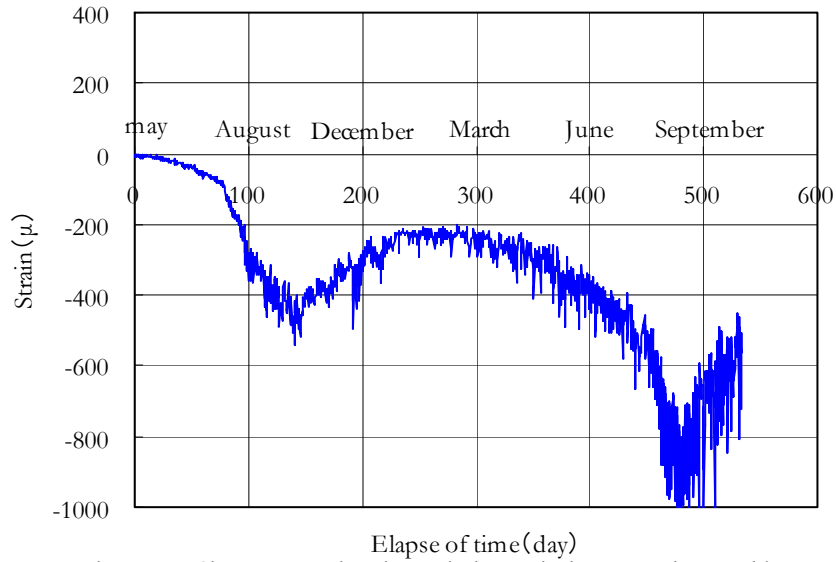


Figure 19: Change over time in strain in vertical prestressing steel bar.

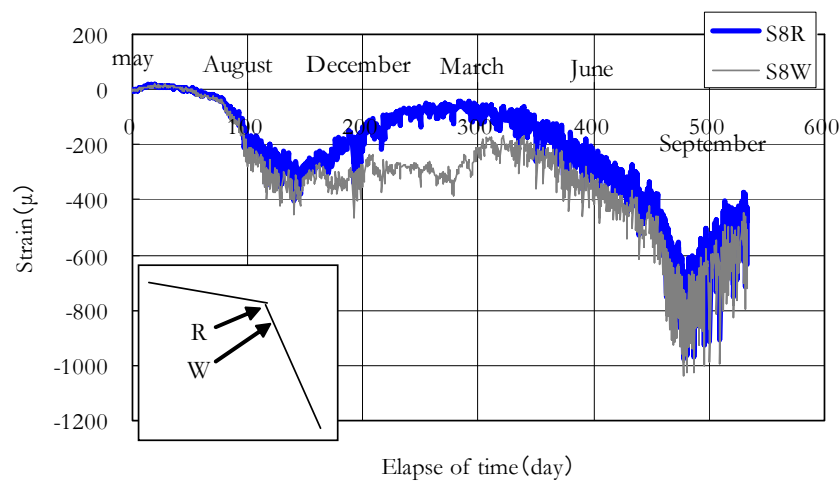


Figure 20: Change over time in strain in steel bar.